Hindawi
Advances in Polymer Technology
Volume 2023, Article ID 9306542, 10 pages
https://doi.org/10.1155/2023/9306542

Research Article

Synthesis, Evaluation, and Electrochemical Detection Application of Magnetic Molecularly Imprinted Polymers for 4,4′-Methylenedianiline from Food-Contact Materials

Lijing Lu,[1,2] **Haoyue Ning**,[1] **Jipeng Guo**,[1] **Chuang Guo**,[1] **Liao Pan**,[1,2] **and Lixin Lu**[1,2]

[1]*Department of Packaging Engineering, Jiangnan University, Wuxi 214122, China*
[2]*Jiangsu Key Laboratory of Advanced Food Manufacturing Equipment and Technology, Wuxi 214122, China*

Correspondence should be addressed to Lixin Lu; lulx@jiangnan.edu.cn

Received 25 February 2023; Revised 11 May 2023; Accepted 23 May 2023; Published 13 June 2023

Academic Editor: Teresa Casimiro

Magnetic molecularly imprinted polymers (MIPs) capable of selectively recognizing and absorbing 4,4′-methylenedianiline (MDA) were successfully synthesized, using Fe_3O_4 coated with mesoporous silicon (Fe_3O_4@$mSiO_2$) as the magnetic carrier, 4-vinyl pyridine (4-VP) as the functional monomer, ethylene glycol dimethacrylate (EGDMA) as the cross-linking agent, and MDA as the template molecule. The morphology, structure, and properties of MIPs were characterized, suggesting that the MIPs had obvious core-shell structure and strong magnetic responsiveness. The results of adsorption property tests showed that the MIPs could specifically recognize and adsorb MDA with excellent selectivity and reusability. The adsorption kinetic process could be described by the pseudo-second-order kinetic model, and the adsorption isotherm could be fitted by the Langmuir model, with a maximum adsorption capacity of 59.5 μmol/g. Furthermore, the magnetic MIPs have been applied to the electrochemical detection of MDA from the composite film sample, with recoveries in the range from 87.8% to 92.5% and the RSD values less than 4.4%. The prepared magnetic MIPs showed potential for the selective separation and detection of MDA in food-contact materials.

1. Introduction

Primary aromatic amines (PAAs) are chemicals with a primary amine -NH_2 attached to an aromatic ring, and several of them have been identified as carcinogens or suspected carcinogens [1]. The sources of PAAs in food-contact materials are varied. Some of them are derived from additives used in the preparation of materials to enhance their properties, for example, 4,4′-methylenedianiline (MDA) added in nylon production [1]. Others are produced by chemical reactions triggered by conditions such as heat and light during storage and use of the materials, among which the two main sources are polyurethane adhesives and azo dyes [2]. Polyurethane is a common component in adhesives, inks, and coatings used to produce flexible food packaging materials, and azo dyes are used as printing ink, paint, and dyeing agent of food-contact materials such as nylon, plastic, and rubber. PAAs, that may migrate from food-contact materials into foodstuffs, can be absorbed by the human body through various ways to harm human health.

Given the toxicity hazard and migration risk of PAAs from food-contact materials, the European regulation on food-contact materials (EU) No. 10/2011 [3] stipulates that the specific "nondetectable" migration limit for each kind of PAAs specified in REACH [4] is 0.002 mg/kg food or food simulants, and the total migration for the PAAs not listed in REACH shall not exceed 0.01 mg/kg food or food simulants. In order to meet the determination requirements for PAAs, many detection methods have been developed [1, 5]. The most commonly used methods are based on spectrophotometry, chromatography, chromatography-mass spectrometry, and direct analysis in real-time mass spectrometry [1, 6]. However, these current methods require high cost (resulting from expensive instruments and performing the assays) and

tedious pretreatment processes (e.g., extraction, purification, and enrichment) due to the complexity of the sample matrix. Additionally, the extraction mediums commonly used in current extraction methods are poorly selective for the target molecules. Therefore, it is essential to develop simple, inexpensive, and efficient methods for the selective separation and accurate determination of PAAs from food-contact materials.

Molecularly imprinted polymers (MIPs) are synthetic polymers with specific recognition sites and strong binding capacities for a given template molecule [7]. MIPs can selectively recognize and absorb the target because of the existing binding sites complementary to the template molecule [8]. Due to their high affinity and selectivity toward templates in complex systems, MIPs show high promise for absorption, separation and purification, biochemistry, and drug delivery [9–11]. Compared with MIPs, magnetic MIPs that use magnetic particles coated by a polymer as the magnetic carrier not only retain the specific recognition ability of MIPs but also have the magnetic characteristic [12]. Hence, they allow a controllable rebinding process and can be more easily separated from sample solution after the recognition and absorption for target molecules. These advantages of specific recognition, rapid separation, and good reusability make magnetic MIP potential in selectively separating and enriching the target molecules from sample matrixes.

Recently, the electrochemical sensors based on MIPs have attracted increasing attention in the determination of diverse target molecules [13]. MIP-based electrochemical sensors are simple and inexpensive and have high sensitivity and selectivity due to the synergic superiorities of electrochemistry and MIPs. Particularly, since the magnetic electrodes are used in electrochemical sensing to capture functionalized magnetic MIPs from sample solutions, the electrochemical detection for target molecules allows excellent electrode regeneration capacity and is more suitable for mass detection [14]. This electrochemical detection method, which is based on the integration of magnetic MIPs and magnetic electrodes, has been used in the separation and detection of metronidazole [15], bisphenol A [16], and mefenamic acid [17]. However, there are rare studies on the potential usage of the magnetic MIPs coupled with magnetic electrochemical sensors to separate and detect PAAs from food-contact materials.

In this paper, the magnetic MIPs for the selective absorption and enrichment of PAAs from food-contact materials were synthesized on the surfaces of magnetic carriers, using MDA (one of the typical PAAs specified in REACH) as the template molecule, 4-VP as the functional monomer, and EGDMA as the cross-linking agent. The synthesis conditions of MIPs were optimized. The morphology, structure, and properties of magnetic MIPs were characterized, and their adsorption properties including adsorption kinetics, adsorption isotherm, selectivity, and reusability were also studied. Finally, the obtained magnetic MIPs were applied in the electrochemical detection by coupling with the magnetic electrodes to achieve the cost-effective, efficient, and sensitive determination of MDA in real samples.

2. Materials and Methods

2.1. Materials. All chemicals were of analytical grade. Nano ferroferric oxide (Fe_3O_4) and tetraethyl orthosilicate (TEOS) were purchased from Shanghai Maclin Biochemical Technology Co., Ltd. (Shanghai, China). 4-Vinylpyridine (4-VP), 4-aminobiphenyl, 4,4′-methylenebis(2-chloroaniline) (MOCA), and 4,4′-methylenebis(N,N-dimethylaniline) were all purchased from Shanghai Aladdin Biochemical Technology Co., Ltd. (Shanghai, China). Ethylene glycol dimethacrylate (EGDMA), 2,2′-azobis(2-methylbutyronitrile) (AIBN), γ-aminopropyltriethoxysilane (KH550), cetyltrimethylammonium bromide (CTAB), 4,4′-methylenedianiline (MDA), isopropanol, anhydrous ethanol, ammonia solution, acetonitrile, anhydrous methanol, disodium hydrogen phosphate, sodium dihydrogen phosphate, and potassium ferricyanide were all purchased from Sinopharm Chemical Reagent Co., Ltd. (Shanghai, China). Single-walled carbon nanotubes were obtained from Nanjing Pioneer Nanotechnology Co., Ltd. (Nanjing, China).

2.2. Preparation of Magnetic Molecularly Imprinted Polymers

2.2.1. Preparation and Surface Modification of Fe_3O_4@mSiO$_2$. The magnetic mesoporous silica carriers were prepared according to the previous report with some modification [18]. The Fe_3O_4 (0.1 g) was activated by HCl solution (1 mol/L) and washed with deionized water to neutrality. The activated Fe_3O_4 particles were dispersed in the mixed solution of anhydrous ethanol (80 mL), deionized water (20 mL), and concentrated ammonia aqueous solution (1 mL). After the obtained mixture was stirred for 0.5 h at room temperature, the TEOS (0.03 g) was added dropwise and stirred vigorously for 12 h. Subsequently, the obtained particles were separated by the applied magnetic field, washed continuously with water and ethanol, and then dispersed in the mixed solution containing water (80 mL) and ethanol (60 mL). After adding CTAB (0.3 g) and concentrated ammonia (2 mL) with stirring for 0.5 h, TEOS (0.4 g) was added dropwise and stirred for 8 h at 70°C. After that, the obtained particles were washed continuously with the ethanol and water and then dispersed in anhydrous ethanol (100 mL) with stirring at reflux for 24 h at 82°C to remove CTAB. After the reaction finished, the products were collected using the applied magnetic field and dried in vacuum at 60°C for 12 h. The obtained magnetic mesoporous silicon carriers were named as Fe_3O_4@mSiO$_2$.

The surface of Fe_3O_4@mSiO$_2$ was modified with the amino groups as the following process. The Fe_3O_4@mSiO$_2$ (0.1 g) was added into isopropanol (100 mL), followed by adding KH550 (150 μL) dropwise with stirring at 82°C. After the mixture was stirred at reflux for 24 h at 82°C, the samples were collected using the applied magnetic field and dried for 24 h. The obtained amino-modified magnetic mesoporous silicon carriers were denoted as Fe_3O_4@mSiO$_2$-NH$_2$.

2.2.2. Preparation of MIPs with Fe_3O_4@mSiO$_2$. The template molecule of MDA (1 mmol) and functional monomer of 4-VP (4 mmol) were dispersed in acetonitrile (25 mL) with stirring magnetically for 3 h to prepolymerize. Afterwards,

the carrier of Fe_3O_4@mSiO_2-NH_2 (0.1 g) and acetonitrile (35 mL) was added with ultrasonically shaking for 10 min, and then, the cross-linking agent of EGDMA (1 mL) and the polymerization initiator of AIBN (50 mg) were added to the above solution. The reaction vessel was sealed after it was filled with N_2 to remove O_2 for 15 min. The polymerization reaction lasted for 24 h at 60°C water bath under the N_2 atmosphere, and the mixture was magnetically separated to obtain the molecularly imprinted polymers with MDA. The resulting products were eluted repeatedly with a solution of methanol and acetic acid (*v*/*v* 9 : 1) in a ultrasonic cleaner (KQ-300DE, Kunshan Ultrasonic Instrument Co., Ltd., China), until no MDA was detected by the ultraviolet spectrophotometer (UV-1800, Shimadzu, Japan) in the solution. The eluted materials were dried in vacuum at 60°C for 12 h to obtain the molecularly imprinted polymers with the template MDA removed, which was named as MIPs (MIPs with Fe_3O_4@mSiO_2). The nonimprinted polymers (NIPs) were prepared under the same conditions without adding MDA.

2.3. Characterizations. The chemical structures of the prepared MIPs were characterized by Fourier transform infrared (FT-IR) spectrophotometer (ALPHA, Bruker, Germany). The morphologies and the elemental analysis of MIPs were characterized by transmission electron microscope (TEM) (JEM-2100, JEOL, Japan) and energy dispersive spectroscopy (EDS) (Talos F200, FEI, America), respectively. The tests were carried out by ultrasonically dispersing the measured samples with ethanol for 10 min, dripping them onto a Cu mesh to dry, and then selecting appropriate magnifications to obtain high-resolution images of the samples. Magnetic properties of MIPs were measured by a vibrating sample magnetometer (VSM) (PPMS-9, Quantum, USA). The adsorption properties of the MIPs were determined by an ultraviolet spectrophotometer (UV-1800, Shimadzu, Japan).

2.4. Absorption Experiments of MIPs

2.4.1. The Effect of Adsorption Time on Adsorption Capacity. In order to study the adsorption kinetics of MIPs for the template MDA, the effect of adsorption time on the adsorption capacity was investigated. 5 mg MIPs were dispersed in 20 mL MDA solution, whose initial concentration was 200 μmol/L. After shaking at 25°C for various time, the magnetic particles in the solution were removed by magnetic separation. The adsorption time was set as 10, 20, 30, 40, 50, 60, 80, 120, 180, and 240 min, respectively. Then, the concentration of residual MDA in the supernatant was determined by ultraviolet spectrophotometer, and the adsorption capacity (q) was calculated according to the following [19]:

$$q = \frac{(C_0 - C_t)V}{m}, \quad (1)$$

where q (μmol/g) is the absorption capacity of MDA, C_0 (μmol/L) is the initial concentration of MDA, C_t (μmol/L) is the concentration of MDA at t min, V (L) is the volume of the solution, and m (g) is the mass of the MIPs.

2.4.2. The Effect of Initial Concentration of MDA on Adsorption Capacity. To study the adsorption isotherms of MIPs for MDA, the effect of initial concentration of MDA on the adsorption capacity was also investigated. 5 mg MIPs were dispersed in 20 mL MDA solutions with various concentrations of 10, 30, 50, 100, 150, 200, 300, 400, and 600 μmol/L. The mixtures were shaken at 25°C for 4 h. Afterwards, the adsorption capacity (Q) in this part was obtained as the same way as Section 2.4.1.

2.4.3. Selectivity and Reusability of MIPs. The selectivity of MIPs was investigated by comparing the adsorption capacity of MIPs for the analogues including MDA, MOCA, 4-aminobiphenyl, and 4,4′-methylenebis(N,N-dimethylaniline). 5 mg MIPs or NIPs were dispersed into 20 mL of above four solutions (200 μmol/L), respectively. After shaking at 25°C for 4 h, magnetic particles were separated from the solutions using the applied magnetic field. The adsorption capacity of MIPs for MDA, MOCA, 4-aminobiphenyl, and 4,4′-methylenebis(N,N-dimethylaniline) was calculated, respectively, following the same way as Section 2.4.1. The selectivity of MIPs was assessed by three parameters including the distribution coefficient (K_d), the selectivity coefficient (k), and the relative selection coefficient (k'), which can be calculated by the following [20, 21]:

$$k_d = \frac{(C_0 - C_e)V}{C_e m},$$
$$k = \frac{K_d(M)}{K_d(N)}, \quad (2)$$
$$k' = \frac{k_{\text{MIPs}}}{k_{\text{NIPs}}},$$

where C_0 and C_e are the initial and equilibrium concentrations of the target molecules in solution (μmol/L), respectively; m is the mass of the adsorbent material (g); V is the volume of the solution (L); $K_d(M)$ and $K_d(N)$ are the distribution coefficients for MDA and other competing molecules (N), respectively; and K_{MIPs} and K_{NIPs} are the selectivity coefficients for the molecularly imprinted and nonmolecularly imprinted materials, respectively.

In order to test the reusability of MIPs for enrichment and separation, the adsorption-desorption procedure was conducted. 5 mg MIPs were dispersed in 20 mL MDA solution (200 μmol/L) and shaken at 25°C for 4 h for adsorption. The adsorption capacity of MIPs for MDA was calculated by the same method above. The MIPs with a saturate accumulation of MDA were collected and washed with a mixture of methanol and acetic acid (*v*/*v* 9 : 1) to remove the template, until no MDA was detected in the eluent. The obtained MIPs were dried and used for the next adsorption experiment. The above adsorption-desorption procedure was repeated several times using the same MIPs.

2.5. Electrochemical Detection Application of MIPs in Real Sample

2.5.1. Preparation of Electrochemical Sensors Based on MIPs. Firstly, the magnetic glassy carbon electrode (MGCE) was pretreated as follows: MGCE was polished with alumina powder and then ultrasonically cleaned with 50% ethanol (v/v) and ultrapure water for 3 minutes successively. After cyclic voltammetry (CV) scanned in 0.1 mol/L H_2SO_4 solution to reach the steady state, the MGCE was scanned in 5 mmol/L solution of $K_3[Fe(CN)_6]/K_4[Fe(CN)_6]$ until the difference in redox potential was less than 90 mV. The MGCE with a clean surface was obtained after dried in nitrogen. Secondly, the MGCE was enhanced sensitivity by drop-coating 5 μL solution of single-walled carbon nanotubes (SWCNTs, 2 mg/mL) onto its surface and then dried by infrared light. Finally, the electrochemical sensor based on MIPs was prepared by the following steps: 2 mg of the prepared MIPs was added into 15 mL MDA solutions with different concentrations and shaken for 60 min to achieve saturate absorption of MDA. And then, the MGCE was immersed into the above solution for 180 s to capture the MIPs onto the MGCE surface. The MGCE was later on removed from the solution and carefully rinsed by distilled water to remove unbound MDA on the surface of electrode. This MGCE modified by MIPs was used for further electrochemical measurements.

2.5.2. Preparation and Measurement of the Real Sample. The multilayer composite packaging film purchased from Wuxi Guotai Colour Printing Co., Ltd. (Wuxi, China) was chosen as the real sample in this experiment. 2.0 g film sample was cut into pieces and then extracted with 40 mL methanol by microwave at 50°C for 15 min. After centrifuged at 5000 r/min for 10 min, the sample solution was obtained for further test.

Electrochemical measurements were performed at room temperature in three-electrode system with an electrochemical workstation (CHI660E, Chenhua Instruments, China). The modified MGCE was used as the working electrode, and the saturated calomel electrode and the platinum wire electrode were used as the reference and counter electrodes, respectively. The electrochemical response was measured using differential pulse voltammetry (DPV) in 0.1 mol/L phosphate buffer solution with the pH of 7. The DPV was performed from 0.2 V to 1.0 V, with the pulse amplitude of 5 mV and the pulse period of 200 ms. In order to ensure clean and smooth electrode surface and eliminate the contaminants and residues from last determination, after each test, the electrode should be pretreated as the process in Section 2.5.1 for the next experiment.

3. Results and Discussion

3.1. Optimization of Preparation Conditions. The chemical bond and binding force between functional monomers and templates directly affected the adsorption capacity of the MIPs for the target molecular [19]. In this study, 4-vinylpyridine (4-VP), α-methacrylic acid (MA), and salicylaldoxime (SA) were selected to evaluate the effects of different functional monomers on the adsorption properties of MIPs. As shown in Figure 1, comparing with the MIPs prepared by functional monomers with the hydroxyl groups (MA, SA), the ones made with 4-VP had higher adsorption capability. This was probably because there were not only hydrogen bonds between the 4-VP and MDA molecules, but also, π-π bonds might had played a role between the two [19]. After saturated adsorption in MDA solution with an initial concentration of 100 μmol/L, the adsorption capacity of MIPs was 37.8 μmol/g, showing excellent adsorption performance. Thus, the 4-VP was used as the functional monomer to prepare MIPs for the following experiment.

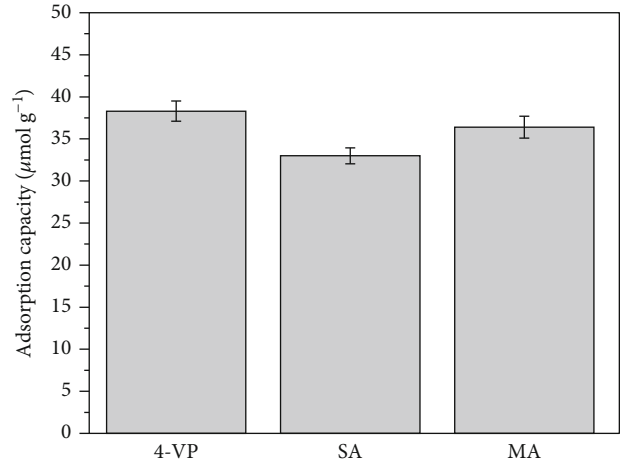

Figure 1: Adsorption capacities of MIPs synthesized by different functional monomers.

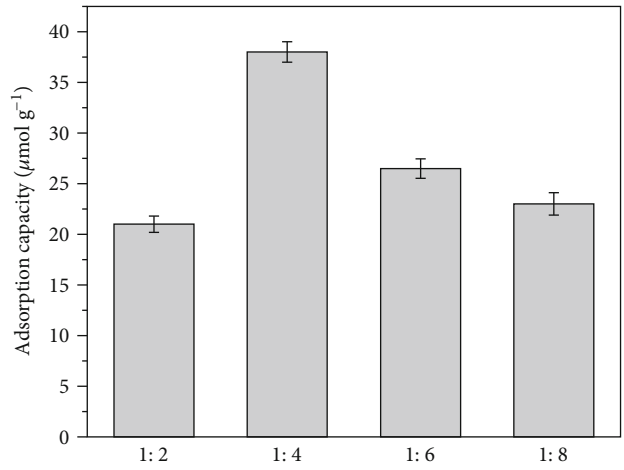

Figure 2: Adsorption capacities of MIPs synthesized by different ratios of templates to functional monomers.

The ratio of template molecules to functional monomers will affect the formation of noncovalent interaction between MIPs and imprinted molecules and further affect the adsorption capability of the MIPs [22]. Four different molar ratios of template molecules (MDA) to functional monomers (4-VP) (1 : 2, 1 : 4, 1 : 6, and 1 : 8) were selected to prepare MIPs, and the adsorption performance was evaluated

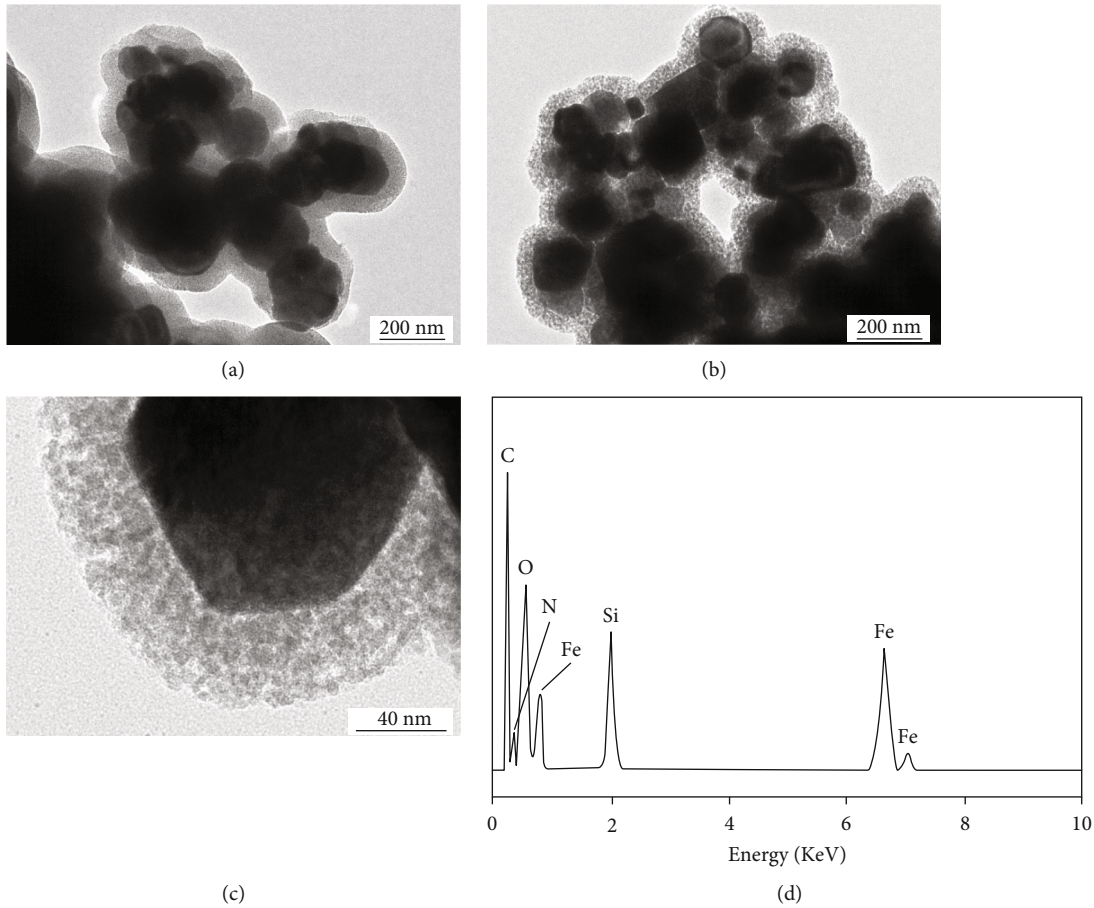

Figure 3: TEM images of Fe_3O_4@$mSiO_2$ (a), MIPs (×20000) (b), MIPs (×100000) (c), and the EDS spectrum of MIPs (d).

through adsorption experiments. It can be seen from Figure 2 that when the molar ratio of template molecules to functional monomers was 1 : 4, the maximum adsorption capacity of MIPs for MDA was obtained, indicating that higher or lower amount of functional monomers will influence the enrichment ability of MIPs. Consequently, the molar ratio of 1 : 4 (template molecules : functional monomers) was selected to prepare the MIPs in this work.

3.2. Characterizations of MIPs. The transmission electron microscopy (TEM) images of the Fe_3O_4@$mSiO_2$ and MIPs together with the EDS spectrum of MIPs are displayed in Figure 3. As seen from Figure 3(a), the Fe_3O_4@$mSiO_2$ was well shaped with particle size of about 230 nm and coated by the hydrolyzed ethyl silicate. This provided the magnetic core with a silica surface, which favored the graft of imprinted polymers [23]. Figures 3(b) and 3(c) show that obvious core-shell structures were emerged in MIPs as darker microspheres Fe_3O_4@$mSiO_2$ were uniformly coated by the imprinted polymers. The particle size of MIPs was a little larger after coated by MDA-imprinted film, and the thickness of imprinted polymer layer was about 40 nm. The polymer shell layers were light gray, and the pore structures could be observed, which suggested that large number of imprinting sites could exist in the imprinted polymer layers to bind the template molecules [24]. This made the recognition sites in the MIPs accessible for the template molecules, and it took shorter time to gain adsorption equilibrium [25]. The EDS (Figure 3(d)) confirmed the presence of iron (Fe), oxygen (O), silicon (Si), and nitrogen (N) in the MIPs suggesting that the polymer shell was successfully coated on the surface of the Fe_3O_4@$mSiO_2$ carrier [7].

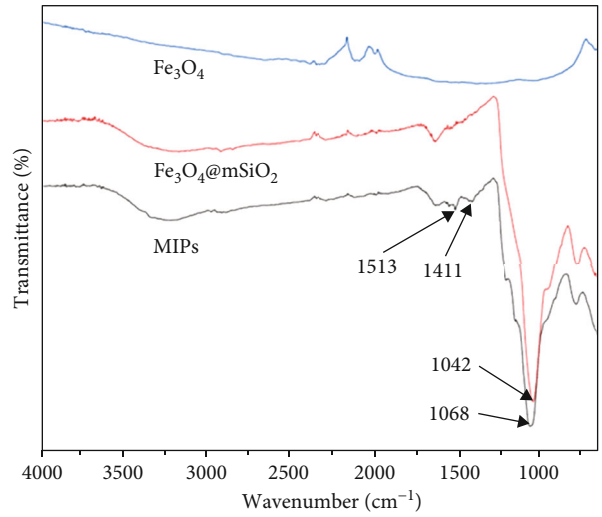

Figure 4: FT-IR spectra of Fe_3O_4, Fe_3O_4@$mSiO_2$, and MIPs.

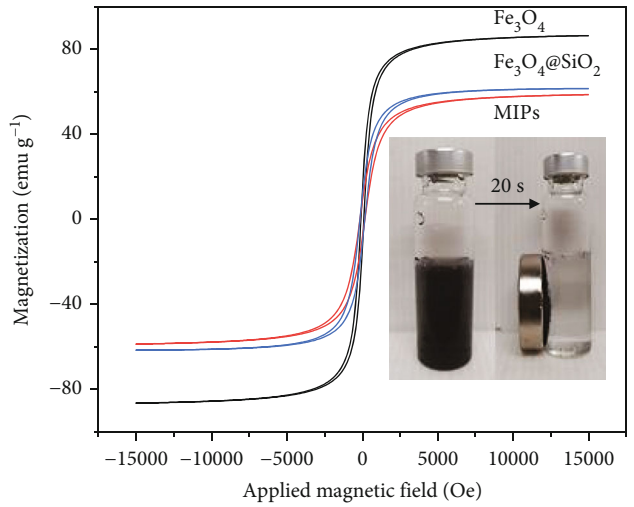

Figure 5: Magnetic hysteresis curves of Fe_3O_4, Fe_3O_4@mSiO_2, and MIPs.

The chemical compositions of Fe_3O_4, Fe_3O_4@mSiO_2, and MIPs were characterized by FT-IR spectroscopy, as shown in Figure 4. Comparing with the infrared spectra of Fe_3O_4, the characteristic peaks at 1042 cm^{-1} and 1068 cm^{-1}, which were attributed to Si–O–Si asymmetric stretching, were observed in the spectra of Fe_3O_4@mSiO_2 and MIPs, respectively. This showed that silica layers were formed on the surface of Fe_3O_4, and thus, the Fe_3O_4@mSiO_2 magnetic carrier was obtained. After coated by imprinted polymer layers, the intensity of Si-O-Si stretching band found in MIPs was significantly weakened. Moreover, the absorption band of C=C bonds at 1411 cm^{-1} and the typical signal of benzene ring structures at 1513 cm^{-1} appeared in the infrared spectrum of MIPs. These results indicated that the imprinted polymer shell was grafted onto the surface of Fe_3O_4@mSiO_2, and MIPs were successfully constructed.

The magnetic properties of Fe_3O_4, Fe_3O_4@mSiO_2, and MIPs were investigated by the hysteresis loops, as depicted in Figure 5. All the magnetization curves were symmetrical, and the saturation magnetization values of Fe_3O_4, Fe_3O_4@mSiO_2, and MIPs are 80.2, 61.1, and 58.6 emu/g, respectively. Although the saturation magnetization value of MIPs decreased in contrast with that of Fe_3O_4 and Fe_3O_4@mSiO_2 to some extent, which ascribed to the magnetic shielding by outer imprinted polymer layers, the MIPs still showed high magnetization. The magnetic MIPs could be fast absorbed to the bottle wall by an external magnetic field without residual magnetism in the solution (inset of Figure 5), demonstrating the excellent magnetic response of MIPs. This magnetic feature made the MIPs potentially useful for separating and enriching targets from sample solutions.

3.3. Adsorption Properties of MIPs

3.3.1. Adsorption Kinetics. The effect of adsorption time on the adsorption capacity of MIPs is exhibited in Figure 6. The adsorption capacity for MDA increased rapidly during the first 40 min, and it reached about 85% of the maximum adsorption capacity. Afterwards, the adsorption rate slowed down gradually with time until the adsorption equilibrium was reached at roughly 80 min, with a maximum adsorption

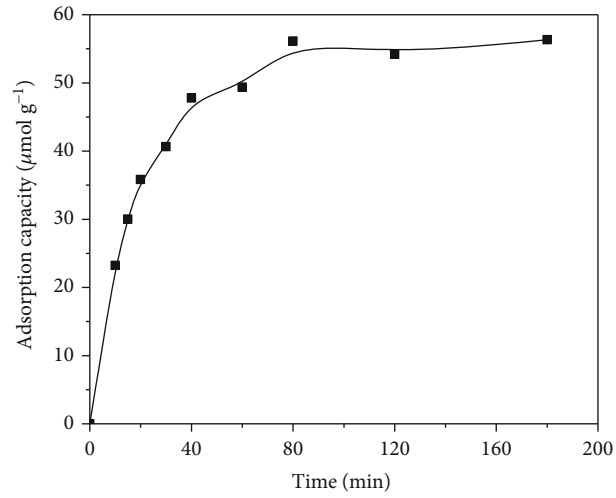

Figure 6: The adsorption kinetic curve of MIPs for MDA.

Table 1: Fitting parameters of pseudo-first-order and pseudo-second-order kinetic models.

$q_{e,max}$ (μmol/g)	Pseudo-first-order model			Pseudo-second-order model		
	k_1	q_e (μmol/g)	R^2	k_2	q_e (μmol/g)	R^2
56.5	0.0300	90.8343	0.5928	0.0015	59.7015	0.9964

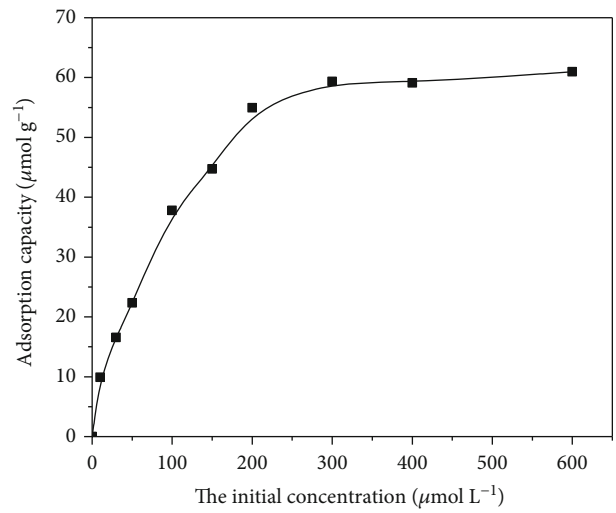

Figure 7: The adsorption isotherm curve of MIPs for MDA.

Table 2: Fitting parameters of the Langmuir and Freundlich models.

$q_{e,max}$ (μmol/g)	Langmuir model			Freundlich model		
	q_{max}	b	R^2	n	K_F	R^2
56.5	71.6332	0.0121	0.9883	2.0759	3.5816	0.9398

Table 3: The coefficients about selectivity of MIPs and NIPs.

Analogues	MIPs		NIPs		k'
	K_d	k	K_d	k	
MDA	54.90	—	19.60	—	—
4-Aminobiphenyl	9.39	5.84	14.72	1.33	4.39
4,4′-Methylenebis(N,N-dimethylaniline)	14.90	3.68	7.84	2.50	1.47
MOCA	24.96	2.20	34.30	0.57	3.86

capacity ($q_{e,\max}$) of 56.5 μmol/g approximately. At early stage of the adsorption process, the concentration of target molecules in solutions was high and lots of binding sites existed on the surface of MIPs, resulting in easy and fast combination between targets and binding sites [26]. The adsorption dynamics was weakened with the reduced concentration of target molecules and available binding sites in later adsorption period, so the adsorption rate of MIPs toward targets declined until the adsorption equilibrium was reached [7].

In order to further investigate the kinetic adsorption process of MIPs, the pseudo-first-order and pseudo-second-order kinetic models were used to fit the experimental data, and the models were defined by the following [27, 28]:

$$\ln (q_e - q_t) = \ln q_e - k_1 t, \qquad \frac{t}{q_t} = \frac{1}{(k_2 q_e^2)} + \frac{t}{q_e}, \tag{3}$$

where q_e (μmol/g) and q_t (μmol/g) are separately the adsorption amounts of MIPs for MDA at equilibrium and time t and k_1 and k_2 are the pseudo-first-order and pseudo-second-order model rate constants, respectively.

The fitting results of the two kinetic models are shown in Table 1. The correlation coefficient ($R^2 = 0.9964$) fitted by the pseudo-second-order kinetic model was much higher than that ($R^2 = 0.5928$) fitted by the pseudo-first-order kinetic model, suggesting that the pseudo-second-order kinetic model could better describe the kinetic adsorption process of MIPs for MDA. Meanwhile, the theoretical adsorption capacity predicted by the pseudo-second-order model was 59.7 μmol/g, which was very close to the measured value of 56.5 μmol/g. Therefore, it could be inferred that the adsorption process between MIPs and targets was mainly chemical interaction.

3.3.2. Adsorption Isotherm. Adsorption isotherm studies are important for estimating the adsorption performance and efficiency of MIPs. Figure 7 shows the relationship between the initial concentrations of MDA solutions and the adsorption capacity of MIPs. When the initial concentration was lower than 200 μmol/L, the adsorption capacity of MIPs enhanced significantly. Subsequently, the adsorption capacity increased slowly with rising concentrations of MDA until it reached stability at MDA initial concentration of 300 μmol/L, which might be because the binding sites on the surface of MIPs were almost completely occupied by MDA and the adsorption saturation was reached [22]. The equilibrium adsorption capacity of MIPs for MDA was 59.5 μmol/g, which was higher than the maximum adsorption capacity of MIPs for MOCA (also one of the typical PAAs) reported in other study [19].

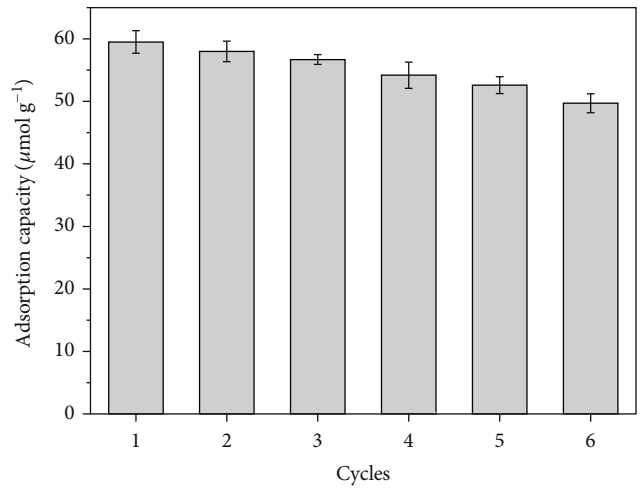

Figure 8: Reusability of MIPs.

The classical Langmuir isothermal adsorption model and the Freundlich isothermal adsorption model were utilized to ulteriorly explore the adsorption mechanism of MIPs. The equations for the Langmuir and Freundlich isothermal models are separately expressed by the following [29, 30]:

$$\frac{C_e}{q_e} = \frac{C_e}{q_{\max}} + \frac{1}{q_{\max} \bullet b}, \qquad \ln q_e = \ln K_F + \left(\frac{1}{n}\right) \ln C_e, \tag{4}$$

where q_e (μmol/g) is the adsorption capacity of MIPs for MDA at equilibrium, C_e (μmol/L) is the equilibrium concentration of MDA solution, $q_{\max}$ (μmol/g) is the maximum adsorption capacity of MIPs for MDA, b represents the Langmuir constant, and K_F and n are the Freundlich constants related to absorption capacity and intensity, respectively.

The adsorption data for MDA onto MIPs were fitted by the Langmuir and Freundlich isothermals, and the results are presented in Table 2. As seen from Table 2, the Langmuir model better fitted the experimental data than the Freundlich model, given that the correlation coefficient of the former ($R^2 = 0.9883$) was higher than that of the latter ($R^2 = 0.9398$). This illustrated that the Langmuir model was more suitable for describing the adsorption behavior

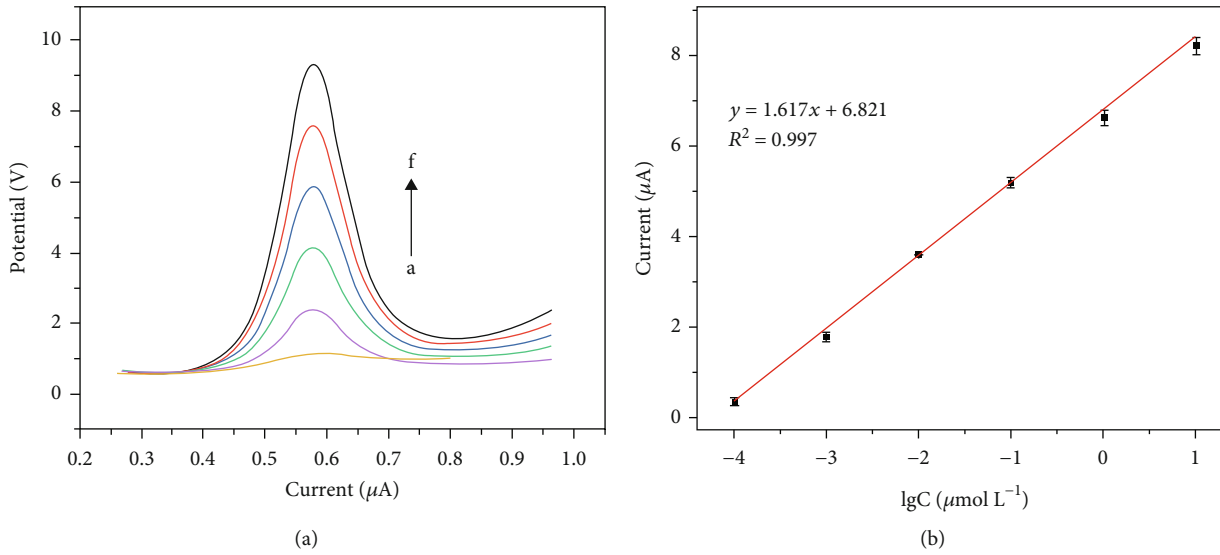

Figure 9: (a) DPV signals of MIP sensors to different concentrations of MDA. (b) The linear relationship of DPV signals and the logarithm of MDA concentrations.

of MIPs, indicating the adsorption process of MDA onto MIPs was mainly monolayer adsorption. The Langmuir model could be used for estimating the adsorption capacity of MIPs in MDA solutions of different initial concentrations due to the well matching with experimental data ($R^2 > 0.98$), and the theoretical value of maximum adsorption capacity obtained by the Langmuir model was 71.63 μmol/g.

3.3.3. Selectivity of MIPs. Three analogues including MOCA, 4-aminobiphenyl, and 4,4′-methylenebis(N,N-dimethylaniline) were selected as competitive molecules to study the selectivity of MIPs for MDA, and the results are shown in Table 3. It can be seen from Table 3 that the k values of MIPs for MOCA, 4-aminobiphenyl, and 4,4′-methylenebis(N,N-dimethylaniline) were 2.2, 5.84, and 3.68, respectively; that was to say, the binding amount to MDA was more than twice of those to other analogues. Thus, it was indicated that the MIPs showed highly selective binding to MDA, which was probably because the specific recognition sites formed on the surface of MIPs better matched with MDA in shapes, sizes, and functional groups [27]. Besides, the adsorption capacity of MIPs for MDA was significantly higher than that of NIPs as the K_d values of MIPs were greater than that of NIPs, suggesting the existence of a large number of specific binding sites for MDA molecules in MIPs. And the k' values were greater than 1 for MIPs. These results confirmed that MIPs had a noticeable imprinting effect and could achieve the selective recognition and absorption for MDA.

3.3.4. Reusability of MIPs. The reusability of MIPs was determined by carrying out the adsorption-desorption experiment. As observed in Figure 8, after repeating the adsorption-desorption process 6 times, the maximum adsorption capacity of MIPs still maintained 83.5% of the initial adsorption capacity. The reduced adsorption capacity might be due to the loss of MIPs in this cyclic procedure [31], but it was not enough to affect the binding capacity of MIPs for MDA. The good reusability and stability allowed the application potential of prepared MIPs in separating and enriching MDA from real samples.

Table 4: Determination results of MDA in real samples ($n = 3$).

Spiked (μmol/L)	Recovery (%)	RSD (%)
0.0	—	—
1.0	87.8	4.4
3.0	90.6	3.2
5.0	92.5	3.0

3.4. Electrochemical Detection Application of MIPs in Real Samples. The response of the electrochemical sensor based on magnetic MIPs to MDA concentrations was performed by DPV, and the results are shown in Figure 9. As seen from Figure 9(a), the DPV signals enhanced gradually with the increase of MDA concentrations. The peak values of current signals had a linear relationship with the logarithm of the MDA concentrations in the range of 0.1 nmol/L to 10 μmol/L, as exhibited in Figure 9(b). The linear regression equation was I_p (μA) = 1.617lg$C$ (μmol/L) + 6.821, and the correlation coefficient (R^2) of the linear fitting was 0.997, favoring the quantitative analysis for MDA. The limit of detection (LOD) for MDA obtained by this method was 0.015 nmol/L ($S/N = 3$), which was much lower than that obtained by the reported method [32]. This may be attributed to the ability of magnetic MIPs to specifically bind and enrich MDA from the solution.

The extracted solutions of composite film samples were spiked with 1.0, 3.0, and 5.0 μmol/L MDA, respectively, and the amounts of MDA were determined by the proposed electrochemical detection method. The results are shown in Table 4. It can be seen that no MDA was detected in the composite film samples, while the recoveries of MDA with three spiked concentrations were 87.8%-92.5% with the

RSD less than 4.4%. Therefore, this method could be used for the detection of MDA from composite film samples.

4. Conclusions

In this work, magnetic MIPs for the specific absorption and enrichment of MDA were synthesized using 4-VP as the functional monomer, EGDMA as the cross-linking agent, and MDA as the template molecule. The morphology, structure, and properties of MIPs were characterized by TEM, FT-IR, and VSM, validating that core-shell MIPs with excellent magnetic responsiveness were successfully constructed. The adsorption properties of the magnetic MIPs were also studied. The results showed that the adsorption kinetics of MIPs for MDA conformed to the pseudo-second-order kinetic model, and the adsorption isotherm accorded with the Langmuir model, with a maximum adsorption capacity of 59.5 μmol/g. Meanwhile, the results of selectivity and reusability tests indicated that MIPs could achieve the specific recognition and absorption for MDA, and they still maintained good recognition and adsorption properties after six adsorption-desorption cycles. Moreover, electrochemical sensors based on the obtained magnetic MIPs were constructed and used to detect MDA from the composite film sample, which provided satisfactory recoveries and RSD values. Thus, the prepared magnetic MIPs could be potentially used for selective separation and electrochemical determination for MDA from food-contact materials.

Data Availability

The data used to support the findings of this study are included within the article.

Conflicts of Interest

The authors declare that they have no conflicts of interest.

Acknowledgments

This work was supported by the National Key Research and Development Program of China (grant numbers 2018YFC1603200 and 2018YFC1603202).

References

[1] X. Trier, B. Okholm, A. Foverskov, M. L. Binderup, and J. H. Petersen, "Primary aromatic amines (PAAs) in black nylon and other food-contact materials, 2004-2009," *Food Additives and Contaminants*, vol. 27, no. 9, pp. 1325–1335, 2010.

[2] G. Campanella, M. Ghaani, G. Quetti, and S. Farris, "On the origin of primary aromatic amines in food packaging materials," *Trends in Food Science and Technology*, vol. 46, no. 1, pp. 137–143, 2015.

[3] The European Commission, "Commission Regulation (EU) No 10/2011 of 14 January 2011 on plastic materials and articles intended to come into contact with food," *Official Journal of the European Commission*, vol. 12, 2011.

[4] The European Commission, *Commission Regulation (EC) No 552/2009 of 22 June 2009 amending Regulation (EC) No 1907/2006 of the European Parliament and of the Council on the Registration, Evaluation, Authorisation and Restriction of Chemicals (REACH) as regards Annex XVII, 552/2009*, Official Journal of the European Commission, 2009.

[5] F. Mohammad, S. Narges, S. Mahboube, and M. M. Masoumeh, "Development of a deep eutectic solvent-based dispersive liquid–liquid microextraction method followed by back-extraction and diazotization coupled to spectrophotometry for determination of total primary aromatic amines from food simulants," *Journal of the Iranian Chemical Society*, vol. 19, p. 3539, 2022.

[6] C. Brede, I. Skjevrak, and H. Herikstad, "Determination of primary aromatic amines in water food simulant using solid-phase analytical derivatization followed by gas chromatography coupled with mass spectrometry," *Journal of Chromatography. A*, vol. 983, no. 1-2, pp. 35–42, 2003.

[7] K. An, H. T. Kang, and D. T. Tian, "Fabrication and evaluation of controllable core/shell magnetic molecular imprinted polymers based on konjac glucomannan for trichlorfon," *Journal of Applied Polymer Science*, vol. 137, no. 30, article 48910, 2020.

[8] T. Y. Zhou, L. Ding, G. B. Che, W. Jiang, and L. Sang, "Recent advances and trends of molecularly imprinted polymers for specific recognition in aqueous matrix: preparation and application in sample pretreatment," *Trends in Analytical Chemistry*, vol. 114, pp. 11–28, 2019.

[9] M. Pourfarzib, R. Dinarvand, B. Akbari-adergani, A. Mehramizi, H. Rastegar, and M. Shekarchi, "Water-compatible molecularly imprinted polymer as a sorbent for the selective extraction and purification of adefovir from human serum and urine," *Journal of Separation Science*, vol. 38, no. 10, pp. 1755–1762, 2015.

[10] S. S. Miao, H. Z. Wang, Y. C. Lu, H. R. Geng, and H. Yang, "Preparation of Dufulin imprinted polymer on surface of silica gel and its application as solid-phase extraction sorbent," *Environmental Science: Processes & Impacts*, vol. 16, no. 4, pp. 932–941, 2014.

[11] W. Du, C. Lei, S. Zhang et al., "Determination of clenbuterol from pork samples using surface molecularly imprinted polymers as the selective sorbents for microextraction in packed syringe," *Journal of Pharmaceutical and Biomedical Analysis*, vol. 91, pp. 160–168, 2014.

[12] H. Jiang, D. L. Jiang, J. D. Shao, and X. L. Sun, "Magnetic molecularly imprinted polymer nanoparticles based electrochemical sensor for the measurement of Gram-negative bacterial quorum signaling molecules (N-acyl-homoserine-lactones)," *Biosensors & Bioelectronics*, vol. 75, pp. 411–419, 2016.

[13] G. Z. Li and K. H. Row, "Applications of magnetic molecularly imprinted polymers (MMIPs) in the separation and purification fields," *Chromatographia*, vol. 81, no. 1, pp. 73–88, 2018.

[14] W. Y. Zhu, L. Xu, C. H. Zhu et al., "Magnetically controlled electrochemical sensing membrane based on multifunctional molecularly imprinted polymers for detection of insulin," *Electrochimica Acta*, vol. 218, pp. 91–100, 2016.

[15] D. Chen, J. Deng, J. Liang, J. Xie, C. K. Hu, and K. Huang, "A core-shell molecularly imprinted polymer grafted onto a magnetic glassy carbon electrode as a selective sensor for the determination of metronidazole," *Sensors and Actuators, B: Chemical*, vol. 183, pp. 594–600, 2013.

[16] L. L. Zhu, Y. H. Cao, and G. Q. Cao, "Electrochemical sensor based on magnetic molecularly imprinted nanoparticles at surfactant modified magnetic electrode for determination of

bisphenol A," *Biosensors & Bioelectronics*, vol. 54, pp. 258–261, 2014.

[17] M. Tayyebeh, H. Esmaeel, and A. Mazaher, "Construction a magneto carbon paste electrode using synthesized molecularly imprinted magnetic nanospheres for selective and sensitive determination of mefenamic acid in some real samples," *Biosensors & Bioelectronics*, vol. 68, pp. 712–718, 2015.

[18] P. P. Yang, Z. W. Quan, Z. Y. Hou et al., "A magnetic, luminescent and mesoporous core-shell structured composite material as drug carrier," *Biomaterials*, vol. 30, no. 27, pp. 4786–4795, 2009.

[19] X. L. Yu, H. Liu, J. X. Diao, Y. Sun, and Y. C. Wang, "Magnetic molecularly imprinted polymer nanoparticles for separating aromatic amines from azo dyes - synthesis, characterization and application," *Separation and Purification Technology*, vol. 204, pp. 213–219, 2018.

[20] A. Ersöz, R. Say, and A. Denizli, "Ni(II) ion-imprinted solid-phase extraction and preconcentration in aqueous solutions by packed-bed columns," *Analytica Chimica Acta*, vol. 502, no. 1, pp. 91–97, 2004.

[21] R. Say, A. Ersöz, H. Türk, and A. Denizli, "Selective separation and preconcentration of cyanide by a column packed with cyanide-imprinted polymeric microbeads," *Separation and Purification Technology*, vol. 40, no. 1, pp. 9–14, 2004.

[22] G. H. Cheng, W. N. Yu, C. Yang et al., "Highly selective removal of 2,4-dinitrophenol by a surface imprinted sol–gel polymer," *Journal of Applied Polymer Science*, vol. 137, no. 41, article 49236, 2020.

[23] Z. H. Zhang, L. J. Luo, R. Cai, and H. J. Chen, "A sensitive and selective molecularly imprinted sensor combined with magnetic molecularly imprinted solid phase extraction for determination of dibutyl phthalate," *Biosensors & Bioelectronics*, vol. 49, pp. 367–373, 2013.

[24] M. Arvand, Z. Erfanifar, and M. S. Ardaki, "A new core@shell silica-coated magnetic molecular imprinted nanoparticles for selective detection of sunset yellow in food samples," *Food Analytical Methods*, vol. 10, no. 7, pp. 2593–2606, 2017.

[25] D. N. Clausen, J. V. Visentainer, and C. R. Tarley, "Development of molecularly imprinted poly(methacrylic acid)/silica for clean-up and selective extraction of cholesterol in milk prior to analysis by HPLC-UV," *The Analyst*, vol. 139, no. 19, pp. 5021–5027, 2014.

[26] W. F. Liu, L. Qin, Z. L. An et al., "Selective adsorption and separation of dibenzothiophene by molecularly imprinted polymer on the surface of porous magnetic carbon nanospheres," *Fullerenes, Nanotubes, and Carbon Nanostructures*, vol. 27, no. 1, pp. 14–22, 2019.

[27] Y. S. Ho and G. McKay, "A comparison of chemisorption kinetic models applied to pollutant removal on various sorbents," *Process Safety and Environment Protection*, vol. 76, no. 4, pp. 332–340, 1998.

[28] Y. S. Ho and G. Mckay, "The kinetics of sorption of divalent metal ions onto sphagnum moss peat," *Water Research*, vol. 34, no. 3, pp. 735–742, 2000.

[29] M. E. H. Ahamed, X. Y. Mbianda, A. F. Mulaba-Bafubiandi, and L. Marjanovic, "Selective extraction of gold(III) from metal chloride mixtures using ethylenediamine N-(2-(1-imidazolyl)ethyl) chitosan ion-imprinted polymer," *Hydrometallurgy*, vol. 140, pp. 1–13, 2013.

[30] S. T. Akar, D. Yilmazer, S. Celik, Y. Y. Balk, and T. Akar, "Effective biodecolorization potential of surface modified lignocellulosic industrial waste biomass," *Chemical Engineering Journal*, vol. 259, pp. 286–292, 2015.

[31] W. T. Zhu, W. T. Li, Z. T. Li et al., "Surface imprinted magnetic carbon nanofibrous microspheres with hierarchical porosity for the highly efficient and selective extraction of brilliant blue from food samples," *Separation and Purification Technology*, vol. 293, article 121128, 2022.

[32] S. K. Mortensen, X. T. Trier, A. Foverskov, and J. H. Petersen, "Specific determination of 20 primary aromatic amines in aqueous food simulants by liquid chromatography-electrospray ionization-tandem mass spectrometry," *Journal of Chromatography. A*, vol. 1091, no. 1-2, pp. 40–50, 2005.